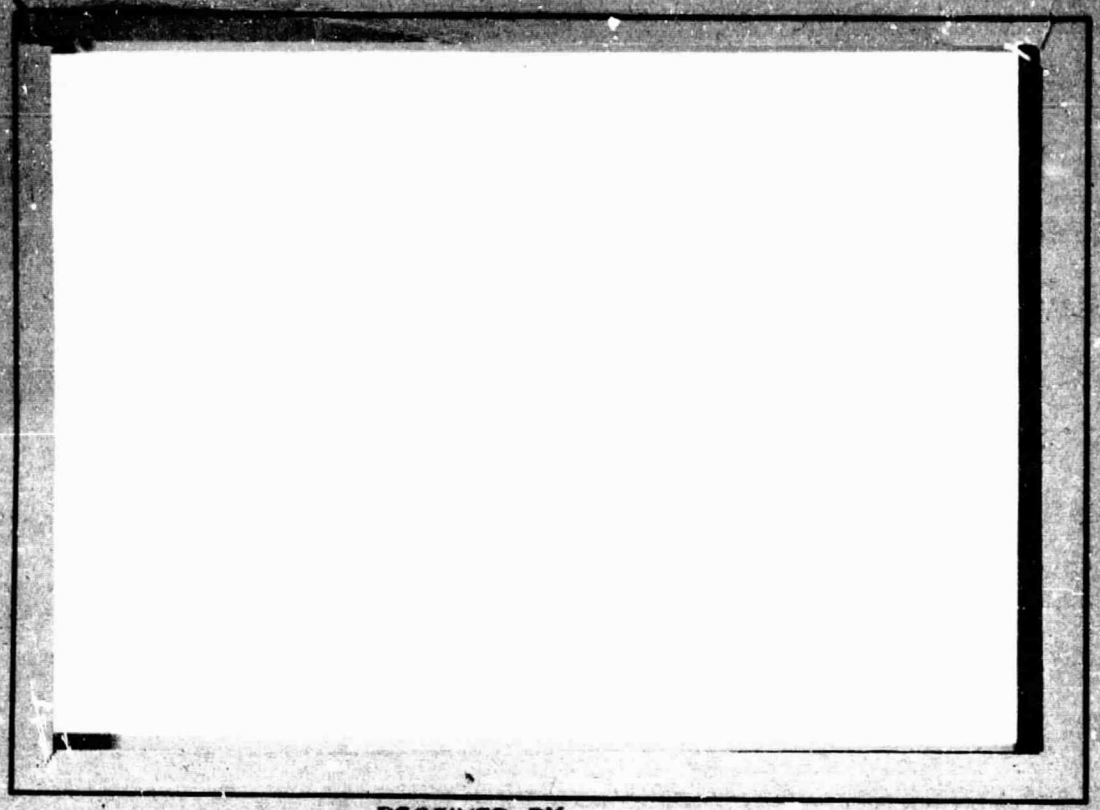

(NASA-CR-174064) COLD STREAMS OF IONOSPHERIC OXYGEN IN THE PLASMA SHEET DURING THE CDAW-6 EVENT OF MARCH 22, 1979 (Consiglio Nazionale delle Ricerche) 30 p
HC A03/MF A01

N85-12513

Unclas
G3/46 02935

ISTITUTO
DI FISICA DELLO SPAZIO INTERPLANETARIO
CONSIGLIO NAZIONALE DELLE RICERCHE
VIA G. GALILEI — 00044 FRASCATI (ITALIA)

COLD STREAMS OF IONOSPHERIC OXYGEN IN THE PLASMA SHEET DURING THE CDAW-6 EVENT OF MARCH 22, 1979.

S. Orsini, E. Amata, M. Candidi
H. Balsiger, M. Stokholm, C. Huang
W. Lennartsson, P. -A. Lindqvist

IFSI-83-15 December 1983

COLD STREAMS OF IONOSPHERIC OXYGEN IN THE PLASMA SHEET DURING THE CDAW-6 EVENT OF MARCH 22, 1979.

S. Orsini, E. Amata, M. Candidi
Istituto di Fisica dello Spazio Interplanetario
CNR, C. P. 27, 00044 Frascati (Roma), Italy

H. Balsiger, M. Stokholm
Physikalisches Institut
University of Bern, 3012 Bern, Switzerland

L. Huang
Dept. of Physics and Astronomy
University of Iowa, Iowa City, Iowa 52243 USA

W. Lennartsson
Lockheed Palo Alto Research Laboratory
Palo Alto, Ca. 94304 USA

P. -A. Lindqvist
Dept. of Plasma Physics
Royal Institute of Technology, 10044 Stockholm, Sweden

Submitted to JGR

IFSI-83-16 December 1983

ABSTRACT

During the March 22, 1979 substorm events the plasma and ion composition experiments in the ISEE-1 and -2 satellites detected cold ionospheric O+ streams, moving tailwards in the near earth magnetotail with the following properties.

1. The streams flow is parallel to the magnetic field lines, with an ExB drift velocity which is in agreement with the electric field topology obtained by mapping the model ionospheric field along the magnetic field lines.
2. Fluctuations of the flow velocity of the streams can be related to magnetotail movements. On the other hand oscillations of the flow direction and speed with periods ranging from 5 to 10 minutes are observed, that suggest the presence of waves.
3. The streams are observed at all distances between 15 Re and 6 Re from the earth. When averaged over 360 degrees the streams show up as a low energy peak, superimposed on the distribution of isotropic plasma sheet ions. This double-peak structure of the energy spectrum seems typical of the disturbed plasma sheet and is possibly related to similar observations made by the GEOS-2 satellite at different local times in the equatorial plane.

INTRODUCTION

For many years one of the most intriguing questions of magnetospheric physics has been the origin of the ions and electrons of the plasma sheet during geomagnetic quiet periods and during active periods. Although new insight into this problem has been gained in the last years, there still exist many unsolved issues.

It is now well known that both solar wind and ionospheric particles contribute to the plasma sheet energetic hot plasma with different rates, which vary according to the global magnetospheric activity (Peterson et al., 1981; Lennartsson et al., 1981). Sharp et al. (1982) pointed out that during active periods ionospheric particles (mainly O+) contribute to the plasma sheet composition by more than 40% in the energy range between 0.1 and 16 Kev, while the solar wind components (H+ and He++) dominate (~95%) during quiet periods.

One open question is still to be answered, concerning the plasma flow pattern between the high latitude ionospheric region where ionospheric ions should be accelerated and solar wind ions are thought to be mirrored and the plasma sheet. Rosenbauer et al. (1975) suggested that the particles, which adiabatically flow tailward along the magnetic field lines, could be drifted towards the central magnetotail axis by the ExB/B' effect.

The ion composition and plasma experiments on board ISEE-1 and -2 satellites detected both O+ and H+ ions, streaming roughly along the magnetic field lines, in the magnetotail lobe region and in the low latitude plasma mantle at 15 - 20 Re distances from the earth (Formisano et al., 1981; Sharp et al., 1981; Candidi et al., 1982; Candidi et al., 1983). These streams have been detected to drift towards the GSM X axis, because of the DC electric field topology present in the tail, so that these could be able to reach the plasma sheet through the boundaries between the plasma sheet and the lobe - plasma mantle regions (Orsini et al., 1982). As a matter of fact, Orsini et al. (1983) observed these streams to cross the boundary and to penetrate in the outher plasma sheet, where another mechanism should energize and thermalize the ionospheric and solar wind particles once they are convected again towards the earth (Pilipp and Morfill, 1978)

In the present study we will report about the observation of these O+ streams inside the plasma sheet and in the lobe region, during the two substorm periods of March 22, 1979, between 15 Re and 6 Re, along the inbound leg of the ISEE satellites orbit. We will show that the streams flow pattern on the GSE XY plane allows to trace the north-south electric field structure in the plasma sheet at various distances in the magnetotail; furthermore we will discuss some fluctuations of the O+ flow velocity and direction which occur during this event, which can help in understanding the magnetotail dynamics during the substorms.

EXPERIMENTS

Data from several experiments have been used in the present study. The technical details for each of them can be found in the literature, as referred in the following.

The main body of data has been taken from the ISEE-2 plasma experiment (PE) (Bonifazi et al. ,1978); the data from the ISEE-1 ion composition experiment (ICE) have been used to identify the ion species (Shelley et al., 1978); electric field data from the ISEE-1 satellite (Mozer et al.,1978) have provided the vector electric field for comparison with the GSE Z component of E as computed from the oxygen ions drift; data from the ISEE-1 LEPEDEA (Frank et al., 1978) have provided information on the three dimensional drift for a cross check of the various data sets; some additional data from the GEOS-2 ICE package (Balsiger et al., 1976) and from the GEOS-2 magnetometer (Candidi et al., 1974) have been used to extend the analysis to a different local time sector.

OBSERVATIONS

Figure 1 shows the GSE and GSM projections of the ISEE-1 and ISEE-2 orbits (together with the orbit of GEOS-2). For the time interval between 1100 UT and 1700 UT, during which oxygen ion streams were observed by the ISEE-2 plasma experiment, the ISEE satellites were inbound between 15 and 5.5 earth radii; in the GSM reference frame X increased from -13 to -4, Y from -7 to -4 and Z decreased from -1 to -3 Earth radii. The satellites explored therefore the southern dawn side near earth magnetotail, and approached the inner edge of the plasma sheet; there was an excursion into the southern lobe region (Manka and McPherron, 1983), as will be evident in the plasma data, between 1406 and 1453 UT.

Typical examples of the appearance of the ion streams in the ISEE-2 plasma experiment data are given in figure 2; each panel shows the intensity of the differential flux (grey shade according to the right side code) of the detected ions as a function of the GSE X and Y components of the equivalent proton velocity, projected into the solar ecliptic equatorial plane; the broken line is the direction of the projection of the ambient magnetic field (courtesy of C. T. Russell, UCLA). In all cases the ions flow direction is close to the magnetic field, with wide fluctuations of the temperature; the upper left panel refers to a detection of a hotter beam than in the upper right panel, and the two lower panels to cases when the beam is cold and the flow direction and energy vary on time scales shorter than the experiment resolution of 96 seconds. In all panels the velocity scale has been limited so that only low energy ions are displayed.

The higher energy plasma sheet population is evident in figure 3, in which the energy per charge spectra are shown for the whole period 1000 UT to 1730 UT. The single plots are averages over 40 minutes of the ISEE-2 plasma experiment data; the left panel is the differential flux integrated over the 180 degrees angular sector including the tailward and dawnward flowing ions; the right panel is the differential flux integrated over the remaining sunward and duskward sectors. All of these (with the exception of the 1410 UT panels) reveal the high energy ions between roughly 100 eV and 10 keV that are the signature of the plasma sheet hot ion population. It is symmetrically distributed between the two panels. After 1121 UT, at low energies and in the left panel only, the cold flowing ions are shown as a distinct peak, that fluctuates in energy and intensity. The single panel at 1410 UT shows a period when ISEE-2 transits into the southern lobe. It is interesting to note that the apparently very uniform signatures in the ions energy and angular distributions are observed while the satellites move earthward between 15 and 5.5 earth radii. From figure 3 it is seen that ISEE-2 is always in the plasma sheet in the period in analysis, except for the 40 minute average 1410 to 1450 UT when

the satellite is located in the plasma lobe; in both regions the streaming particles are observed.

The low energy peaks in the left panels of figure 3 are due to cold ions that are identified to be oxygen ions by a comparison with the corresponding ISEE-1 ICE data during the same period. This comparison is shown in figure 4 which also displays the GEOS-2 ICE data for the same time intervals. The upper panels are again averages (over different time ranges with respect to figure 3) of the ISEE-2 plasma experiment data, the ISEE-1 ICE data are displaied for comparison in the middle panels. In both cases the ICE data reveal that the low energy ions are predominantly oxygen ions, while the hot plasma sheet component is predominantly made of protons. There is a slight difference between the energy of the oxygen ions measured by the two instruments; this is consistent with the fact that the two satellites are located at GSE X positions that differ by 2 to 3 earth radii, while the Y and Z coordinates are much closer; in this configuration it is expected that ions detected at ISEE-1, that is trailing, should have higher energies than those detected at ISEE-2, that is leading (Candidi et al., 1982). In fact, due to the dawn to dusk magnetotail electric field, ions flowing from the ionosphere towards the magnetotail on high latitude magnetic field lines will be subject to a drift perpendicular to B. The flow direction of the streams results from the vectorial sum of the ExB/B drift velocity and the parallel velocity; because this latter depends on energy, the higher energy ions will flow at smaller drift angles than the lower energy ions and they will be driven into the equatorial plane at larger distances from the earth than the lower energy ions (Rosenbauer et al., 1975). In the case considered the energy dispersion is higher than what expected and this would imply higher than usual cross tail electric fields. The lower panels of figure 4 show the GEOS-2 ICE data for the same UT time periods. In these we notice a high energy hot ion population (mainly composed of protons in the left panel and of oxygen ions in the right panel), and a low energy population that again is composed of oxygen and protons. It is very intriguing that oxygen shows up as the dominant species at low energies both at GEOS-2 and at ISEE-2, altough the two spacecrafts are at a very different local time and distance from the earth.

Figure 5 shows the angular distributions of the GEOS-2 low energy oxygen ions from lower (bottom) to higher energies (top in the figure) for two spin scans pertaining to the time periods in the lower panels of figure 4. The angular distribution of the counts in the lowest energy channel (ranging from 4 to 130 eV) is not isotropic, while the angular distributions of the higher energy oxygen ions are. This different angular distributions suggest that we are observing at GEOS-2 the same double population as at ISEE; at low energy we detect ionospheric oxygen that is flowing roughly along the magnetic field, while at higher energy we detect isotropic plasma typical of the plasma sheet. The

GEOS-2 magnetic field at these times is highly distorted and inclined 55 to 45 degrees with respect to the satellite spin axis, i. e. 45 to 35 degrees above the satellite equatorial plane. In this configuration the ICE instrument, which accepts ions flowing within 20 degreees of the satellite equatorial plane, allows the oxygen ions to be detected when flowing with a drift angle to the magnetic field direction between 25 and 35 degrees. The energies are lower at GEOS-2 than at ISEE; this could be explained by the same velocity filter already mentioned as GEOS-2 is much closer to the earth and to the magnetic equator than ISEE during the two time periods considered.

DATA ANALYSIS

Having identified the ion species detected at ISEE-2 as oxygen, we can proceed to the computation of its density, velocity and temperature, and of the flow directions; they are shown in figure 6, together with the GSE Z component of the ambient electric field as computed under the assumpion that E+vxB=0. The ISEE-2 magnetic field is plotted as well, and the depression of theta to zero between 1350 UT and 1430 UT confirms that we have really transited into the southern lobe (phi is around -150 degrees, indicating a tailward field). The large error bars on some of the plasma experiment data points are the effect of the width of the dawnward angular sector (90 degrees); when the oxygen ion beam is detected there it is impossible to determine the flow direction to better than a 45 degrees accuracy; this large error bar reflects on all the derived parameters errors. In some instances, during these periods of large error, some measurements may fall in the high angular resolution sectors, due to fluctuations of the electric field and the consequent fluctuations of the drift velocity, so that better defined measurements are present; these give an indication of the real values for the poorly determined periods as well. This may be the case for the plot of the GSE Z component of the ambient electric field, after 1530 UT, when it would hardly be possible to even state that the polarity is defined, were it not for the few values that have a smaller error, which are definitely positive. This can be checked by comparison with Ez as evaluated, on a less refined time scale, from the ICE data, in figure 7. These values generally follow the same trend of those derived from the plasma experiment.

The comparison of the parameters, as derived from the two instruments, confirms the correct identification of the ion species. In fact the time history of the oxygen ions parameters as derived from the ICE data is the same as that of the parameters of the ions detected by the plasma experiment, when computed under the assumption that they be oxygen ions. The flow velocity varies between extremes of 20 km/sec (i.e. the velocity of oxygen ions detected in the lowest energy channel of the plasma experiment), and a maximum of 120 km/sec. We see from figure 6 that the flow velocity is generally directed tailward and towards dawn; the direction of flow is obviously meaningful only with respect to the magnetic field, and this is shown in the VYMF plot; this component of the flow velocity across the magnetic field is generally positive, indicating a flow direction away from the center of the magnetotail, as expected in the plasma sheet (see Orsini et al., 1983), and only shows negative values when the satellites are located in the plasma lobe, 1406 UT to 1453 UT, indicating there the usual flow towards the center of the magnetotail. Neither the plasma experiment data nor the ICE data allow the determination of the flow direction elevation out of the ecliptic plane; this is made possible by using the

plasma data collected on ISEE-1 by the LEPEDEA experiment. In figure 8 examples of the LEPEDEA data are shown; the upper left and lower right panels refer to periods when the fluctuations of the beam parameters were faster than the experiment time resolution; the data shown in the other panels are not time aliased. They show a low energy ion stream in the 5P and 6P angular sectors, i. e. detector look angle towards the South, and beam direction from the South to the North, in agreement with the expectation for the drift of a southern magnetotail beam in the presence of a dawn to dusk electric field. The data in the upper left panel refer to 1120 UT, close to the neutral sheet, when we may expect a more dynamic behavior. The lower right panel data are taken around a transition between the plasma sheet and the lobe and the energy of the stream varies across this boundary in less than the eight minutes resolution of the measurement.

Figure 9 shows a comparison of the Ez GSE component of the electric field computed from the plasma experiment data and from the ICE data, with the same Ez computed, under the assumption that E.B=0, from the Ex and Ey components measured by the electric field experiment on ISEE-1. The agreement between the three plots appears to be good. Two interesting features can be identified, at 1450 UT and from 1500 to 1510 UT. A sharp transition of Ez from negative values to positive values is observed at 1450 UT at both spacecrafts. A large positive fluctuation of Ez is observed on ISEE-1 between 1500 UT and 1510 UT. The fact that nothing similar is detected by means of the plasma experiment on ISEE-2 may be attributed to the spatial separation between the two spacecrafts.

SUMMARY AND DISCUSSION

In this final section we will summarize and discuss the three main topics dealt with in the paper: electric field topology in the magnetotail versus mapping models of the field from the ionosphere; oscillations of the O+ streams parameters and movements of the tail; streams distributions in the tail versus distance from the earth and local time.

As regards the first topic, we recall that, as shown in the preceeding sections, cold O+ streams are present throughout the CDAW-6 event of March 22, 1979, from 1120 UT to 1715 UT, during which at least two major substorms occurred, respectively starting at 1030 UT and at 1330 UT (Manka and McPherron, 1983). The ISEE-2 satellite was in the plasma sheet from 1000 UT (and before this time as well) to 1406 UT and from 1453 onwards; from 1406 UT to 1453 UT it was in the southern lobe. Throughout the period, the streams flow almost parallel to the magnetic field lines and are subject to an ExB drift. We recall that the model for the tail electric field obtained by mapping E along the magnetic field lines up from the ionosphere (Rostoker and Bostrom, 1976) predicts Ez to be positive in the southern dawn plasma sheet, and negative in the southern dawn lobe (figure 11). This fact is confirmed by the data in the whole period that we have studied, as shown in figures 6, 7, 9 and 10. Actually, Ez, as computed from various experiments on ISEE-1 and ISEE-2, is generally negative or fluctuates around zero in the lobe period, from 1406 UT to 1453 UT; on the contrary, it is positive during the periods when the satellites are in the plasma sheet.

The sign reversal at the boundary is not clearly seen for the 1406 UT plasma sheet boundary crossing because of a lack of data and the presence of oscillations of Ez; instead, the crossing neatly shows up in the data at 1453 UT as a fast change of the Ez polarity both at ISEE-1 and ISEE-2 within one minute (see figs. 8 and 10), when the two satellites are at 3 Re distance in XGSE, but quite close to each other in the YGSE component. We conclude that our observations fit nicely with the predictions of the mapping model.

We shall now turn our attention to the fluctuations of the O+ streams parameters. As already mentioned in the discussion of figure 6, the O+ flow velocity fluctuates through the whole period. In order to interpret such fluctuations, it is necessary to evaluate the relevance on the data of the satellites motion along their orbit. The effect of this motion, moving from the tail towards the earth, is expected to be twofold: a slow decrease due to the ExB drift filter, which lets higher energy ions fall towards the tail axis farther from the earth than the lower energy ones, and a slow increase because the distance from the neutral sheet Z' (Fairfield, 1980) increases as the satellites move towards the earth (see figure 3); also in this latter case the effect is due to the ExB filter which predicts the observations of higher energy ions farther from the neutral she-

et. Neither mechanism can explain the fast fluctuations displayed in figure 6 and 10. A possible interpretation of the oscillations is that they are a consequence of variations of the ionospheric source of the oxygen streams. We do not think that this is the case because B and Ez, that are local parameters, oscillate just when the flow velocity does (figs. 6 and 10); it is difficult to believe that this occurs by chance or that there is a common origin for the oscillations of the ionospheric source and of fields in the tail. Instead, we propose two possible scenarios. The first is that rigid movements of the magnetotail cause a change of its position relative to the satellite; the high velocity periods would correspond to observation points which are more distant from the central axis of the tail than the low velocity periods. The second possible scenario is that non rigid compressions of the whole magnetotail move the satellite on field lines that are closer to the magnetopause. In both cases the velocity fluctuations would be an effect of the ExB filter action on the O+ streams flow patterns.

Wave-like profiles appear during the period between 1330 UT and 1530 UT (figs. 6 and 10), at the onset of the second substorm. They suggest that waves may be propagating through the magnetotail during the major substorm phase. The velocity fluctuations are particularly large (about 40 Km/s peak to peak) in the region just outside the lobes, between 1330 UT and 1406 UT and between 1450 UT and 1530 UT, with periods closed to 15 minutes in the first case and close to 10 minutes in the second (figs. 6 and 10). On the contrary the direction does not fluctuate as dramatically as the total speed. A hint of small fluctuations can be seen, during the same two periods, in the Ez plot, but the large error bars do not allow any firm conclusion. The observations are much neater in the lobes, especially soon after 1406 UT and presumably close to the boundary. From 1406 UT to 1453 UT Ez, which was positive in the plasma sheet, is steadly negative or fluctuates around zero. Two oscillations of the flow direction (45 degrees peak to peak) are clearly seen in the lobes (figure 10, 1406 UT to 1425 UT), which are in phase with fluctuations of the magnetic field, both in value and in elevation.

Further evidence for magnetotail movements relative to the satellites can be obtained from the 1453 UT boundary crossing. Actually, the simultaneous detection of the Ez reversal at the two satellites, together with the increase of the O+ flow velocity as the satellites sample the plasma sheet, is consistent with a motion of the plasma sheet boundary mainly in the YZ GSE direction. Throughout the lobe traversal period the velocity is low. This indicates that in the lobe region the satellites are closer to the central magnetotail axis than when in the plasma sheet; this would imply that the whole magnetotail has moved in such a way as to reduce the distance of the satellite from the central magnetotail axis, while the plasma sheet thinned and caused the satellites to transit into the lobes. The fast

increase of the O+ streams flow velocity at 1453 UT, which is correlated with the plasma sheet appearence, would thus be correlated again with the movement of the plasma sheet boundary, during the substorm recovery phase.

The observations of the oxygen streams at the ISEE satellites between 1130 UT and 1715 UT implies that the ionosphere has been continously accelerating these ions during the substorm events as well as several hours after their onsets. It indicates that the mechanism accelerating these ions is not directly correlated with the substorm (see Lui et al., 1983), altough it seems that the substorm triggers it or that during the substorm it becames more efficient.

Finally we want to discuss the dependence of the streams characteristics on the distance from the earth and from the magnetic equator. As it has been shown in figures 3 and 4, the streams show up as a peak in the low energy range of the energy spectra. The peak is observed, together with the plasma sheet hot plasma, by ISEE-2, travelling towards to the earth in the dawn side of the tail, south of the tail neutral sheet, as well as by GEOS-2, which is moving on the dusk portion of the geosyncronous orbit, close to the GSM XY plane. No local time dependence is evident from the data analyzed. It seems indeed that the energy of the streams decreases as the distance from the magnetic equator and from the earth decreases, because of thw ExB drift filter mechanism (see figure 4). In the case these oxygen streams are thermalized and convected towards the earth once they get to the neutral sheet, we should observe higher abundances of plasma sheet oxygen when moving from high latitudes (and higher distances from the earth) to low latitudes (and lower distances from the earth). This is evident in the hot plasma sheet population, when comparing the simultaneous ISEE-1 and GEOS-2 ion compositions, as shown in figure 4, in the middle and bottom right panels. In principle this mechanism could explain the high hot O+ abundances, frequently observed at the inner edge of the plasma sheet (Balsiger, 1983).

ACKNOWLEDGEMENTS

We thank C. T. Russell for providing the ISEE magnetic field data. We thank A. Ghielmetti for the computation of the O+ parameters from the ISEE-1 ICE data. We thank G. Paschmann for useful discussions on evaluating the data.

Part of this work was supported by the Swiss National Foundation, grant ..... Part of this work was supported by NASA contracts NAS5-26257 and NAS5-25530, grant NGL16-001-002 and Office of Naval Research contract N00014-76-C-0016.

One of us (S. O.) was allowed by an E.S.A. felloship c/o the Physikalisches Institut of the University of Bern (Switzerland) when analyzing the data for this paper.

FIGURE CAPTIONS

Figure 1: GSE and GSM projections of the inbound and outbound legs of ISEE-1 and ISEE-2, together with the geosyncronous orbit of GEOS-2, rotated on the GSE XY plane, for the CDAW-6 event of March 22, 1979.

Figure 2: ISEE-2 plasma experiment data plotted as differential flux (log(cm2*s*sr*keV)-1, according to the grey shade code as shown on the right hand side) versus the equivalent proton velocity of the ion. Vx and Vy in the GSE system are plotted along the vertical and horizontal axes in km/sec. The broken line is the projection of the ambient magnetic field. The four panels are data accumulated over 96 second at different UT times.

Figure 3: Plasma experiment ion differential flux (cm2.s.sr.kev)-1 versus energy per charge. Averages over 40 minutes are plotted, with time and satellite GSE and GSM position listed on the right side (R=distance, LT=local time, LAT=elevation; LATZ' is the artificial elevation of the satellite, assuming ZGSM=Z', the estimated distance from the neutral sheet (Fairfield, 1980)). The right hand panels are integrated over the 180 degrees, corresponding to sunward and duskward flowing ions, while the left hand panels are integrated over the antisunward and dawnward flow directions. The isotropic population at high energy is the plasma sheet plasma, and the lower energy ions present in the left hand panels only are the oxygen ions flowing tailwards along the magnetic field lines.

Figure 4: Two plasma experiment energy spectra averaged over 40 minutes (top panels) are compared with the corresponding data from ISEE-1 ICE (middle panels); the high energy population between several hundreds of eV and 11 keV consists of plasma sheet protons, while the low energy peak is mainly composed of oxygen ions. The lower panels show GEOS-2 ICE energy spectra for the same UT periods. These reveal, at 6.6 Re and in the equatorial afternoon local time sector, the same general structure in the ion composition; higher energy ions with a low energy component.

Figure 5: Angular distributions of the oxygen ion count rates for 16 energy steps (4 eV - 16 KeV) as detected by the GEOS-2 ICE. Two scans are shown, each taken during one of the UT periods of the spectra given in the bottom

panels of figure 4. The low energy ions are not isotropic, while the higher energy ions are. The values of the GSE and GSM components of the ambient magnetic field are indicated.

Figure 6: Oxygen ions parameters as computed from the plasma experiment data. From the bottom: density (cm-3), flow velocity (Km/s), XY GSE flow direction (degrees), thermal velocity (Km/s), flow direction with respect to the magnetic field GSE XY projection, the components of the GSE XY flow velocity parallel and orthogonal to the magnetic field (VXMF,VYMF) and the GSE Z value of the electric field (computed under the assumption E=-vxB). The top three panels show the ISEE-2 GSE polar coordinates of the magnetic field (absolute value, longitude and latitude). The satellite GSE position (local time, distance and latitude) is indicated at the bottom. The large error bars in the parameter plots are due to the ion beam being detected in the wide angular sector.

Figure 7: Same as figure 6 for the ISEE-1 ICE oxygen data. The energy range up to 7 keV has been chosen, since no streams are present at higher energies. The thermal energy is plotted in KeV units.

Figure 8: ISEE-1 LEPEDEA data for four selected times during the event. In each panel, the individual frames relate to ions, labelled P, and electrons, labelled E, for different look elevation ranges from 90 degrees (frame 1) to -90 degrees (frame 7). In each frame count rates are grey shade coded versus look longitude (-180 to 180 degrees), and versus energy (1 eV to 45 keV).

Figure 9: Ez GSE component of the ambient electric field as measured by three different techniques: the ISEE-1 DC electric field experiment under the assumption E.B=0 (left), the ISEE-2 plasma experiment oxygen ion parameters (middle) and the ISEE-1 ICE experiment oxygen ion parameters (right) under the assumption that E+vxB=0.

Figure 10: Detailed plots of some oxygen parameters as measured by the ISEE-2 plasma experiment for the periods of wave like trends observation. From the bottom: density (cm-3), flow velocity (Km/s), flow direction in respect to the magnetic field GSE XY projection, GSE Z component of the elctric field (computed under the assumption E=-vxB), ISEE-2 magnetic field (absolute value, GSE longitude and latitude).

Figure 11: GSM YZ projection of the electric field topology at 8 Re from the earth (Rostoker and Bostrom, 1976). The mark indicates the ISEE-2 position at 1500 UT, when the plasma sheet boundary was crossed.

REFERENCES

Balsiger H., P. Eberhardt, J. Geiss, A. Ghielmetti, H. P. Walker, D. T. Young, H. Loidl and H. Rosenbauer, A satellite borne ion mass spectrometer for the energy range 0 to 16 keV, Spa. Sci. Instrum., 2, 499, 1976.

Balsiger H., On the composition of the ring current and the plasmasheet and what it tells about the sources of these hot plasmas, High Latitude Plasma PHYsics, Ed. by B. Hultqvist and T. Hagfors, Plenum Press, 313, 1983.

Bonifazi C., P. Cerulli-Irelli, A. Egidi, V. Formisano and G. Moreno, The EGD positive ion experiment on the ISE-E-B satellite, IEEE Trans. Geosci. Electron., GE-16, 243, 1978

Candidi M., R. Orfei, F. Palutan and G. Vannaroni, FFT analysis of a spac magnetometer noise, IEEE Trans. Geosci. Elec., GE-12, 23, 1974.

Candidi M., S. Orsini, Estimates of the North-South electric field component in the magnetotail low latitude boundary layer, Geophys. Res. Lett., 8, 637, 1981.

Candidi M., S. Orsini and V. Formisano, The properties of ionospheric O+ ions as observed in the magnetotail boundary layer and northern plasma lobe, J. Geophys. Res., 87, 9097, 1982.

Candidi M., S. Orsini and A. Ghielmetti, Observation of multiple ion streams in the magnetotail low latitude boundary layer. Evidence for a double H+ population, Accepted by J. Geophys. Res., 1983.

Fairfield D. H., A statistical determination of the shape and position of the geomagnetic neutral sheet, J. Geophys. Res., 85, 775, 1980.

Formisano V. , S. Orsini and M. Candidi, Observation of ionospheric oxygen in the geomagnetic tail by ISE-E-2, Adv. Space Res., 1, 313, 1981.

Frank L. A., D. M. Yeager, H. D. Owens, K. L. Ackerson and M. R. English Quasispherical LEPEDEAS for ISEE's-1 and -2 plasma measurements, IEEE Trans Geosci. Electon., GE-16, 221,1978.

Lennartsson W., R. D. Sharp, E. G. Shelley, and R. G. Johnson,

Ion composition and energy distribution during 10 magnetic storms, J. Geophys. Res., 86, 4628, 1981.

Lui A. T., T . E. Eastmann, D. J. Williams, and L. A. Frank, Observations of ion streaming during substorms, J. Geophys. Res., 88, 7753, 1983.

Manka R. H. and R. L. McPherron, Dynamics of the March 22, 1979, substorm event: CDAW-6, submitted to J. Geophys. Res., this issue, 1983.

Mozer F. S., R. B. Torbert, U. V. Fahleson, C. G. Falthammar, A. Gonfalo and A. Pedersen, Measurements of quasi-static and low frequency electric fields with spherical double probes on the ISEE spacecraft, IEEE Trans. Geosci. Electron., GE-16, 258, 1978

Orsini S., M. Candidi, H. Balsiger and A. Ghielmetti, Ionospheric ions in the near earth magnetotail plasma lobes, Geophys. Res. Lett., 9, 163, 1982.

Orsini S., M. Candidi, V. Formisano, H. Balsiger, A. Ghielmetti and K. W. Ogilvie, The structure of the plasma sheet - lobe boundary in the earth's magnetotail, accepted by J. Geophys. Res., 1983.

Peterson W. K ., R. D. Sharp, E. G. Shelley, R. G. Johnson and H. Balsiger, Energetic ion composition of the plasma sheet, J. Geophys. Res., 86, 761,1981.

Pilipp W. G. and G. Morfill, The formation of the plasma sheet resulting from plasma mantle dynamics, J. Geophys. Res., 83, 5670, 1978.

Rosenbauer H. , Grunwaldt, M. D. Montgomery, G. Paschmann and N. Sckopke, HEOS 2 plasma observations in the distant polar magnetosphere, J. Geophys. Res., 80, 2723, 1975.

Sharp R. D., D. L. Carr, W. K. Peterson and E. G. Shelley, Ion streams in the magnetotail, J. Geophys. Res., 86, 4639, 1981.

Sharp R. D., W. Lennartsson, W. K. Peterson and E. G. Shelley, The origin of the plasma in the distant plasma sheet, J. Geophys. Res., 87, 10420, 1982.

Rostoker G. and R. Bostrom, A mechanism for driving Birkeland current configuration in the auroral oval, J. Geophys. Res., 81, 235, 1976.

Shelley, E. G ., R. D. Sharp, R. G. Johnson, J. Geiss, P. Eberhrdt, H. Balsiger, G. Haerendel and H. Rosenbauer, Plasma composition experiment on ISE-E-A, IEEE Geosci. Electron., GE-16, 266, 1978.

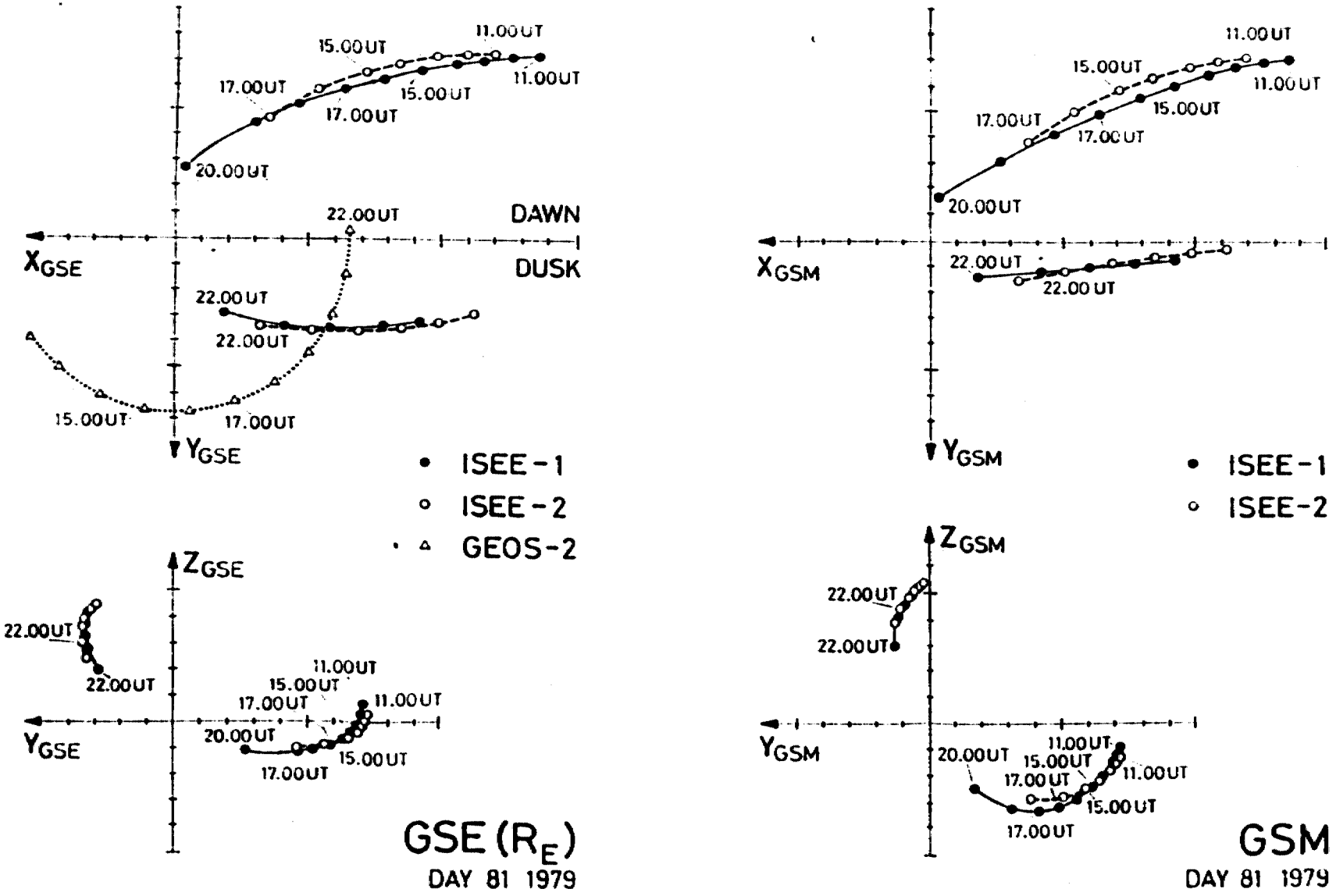
11.00UT
15.00UT
17.00UT
11.00UT
15.00UT
17.00UT
20.00UT
22.00UT
DAWN
X_{GSE}
DUSK
22.00UT
22.00UT
15.00UT
17.00UT
Y_{GSE}
• ISEE-1
○ ISEE-2
△ GEOS-2
Z_{GSE}
22.00UT
22.00UT
11.00UT
15.00UT
17.00UT
11.00UT
Y_{GSE}
20.00UT
15.00UT
17.00UT
GSE (R_E)
DAY 81 1979
11.00UT
15.00UT
17.00UT
11.00UT
15.00UT
20.00UT
22.00UT
X_{GSM}
22.00UT
22.00UT
Y_{GSM}
• ISEE-1
○ ISEE-2
Z_{GSM}
22.00UT
22.00UT
Y_{GSM}
20.00UT
11.00UT
15.00UT
17.00UT
11.00UT
15.00UT
17.00UT
GSM
DAY 81 1979

Figure 1

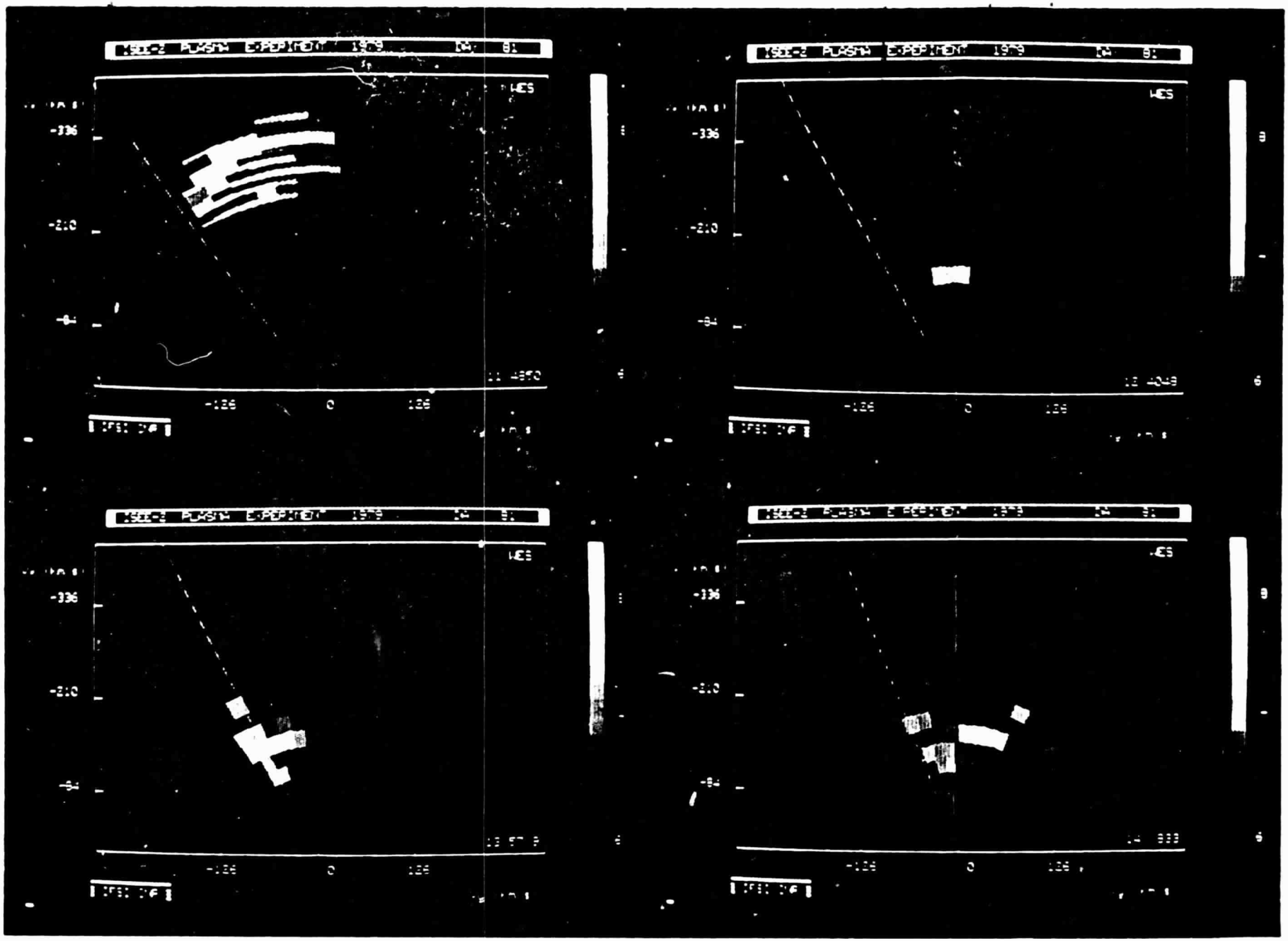
-336
-210
-84
-126
0
126

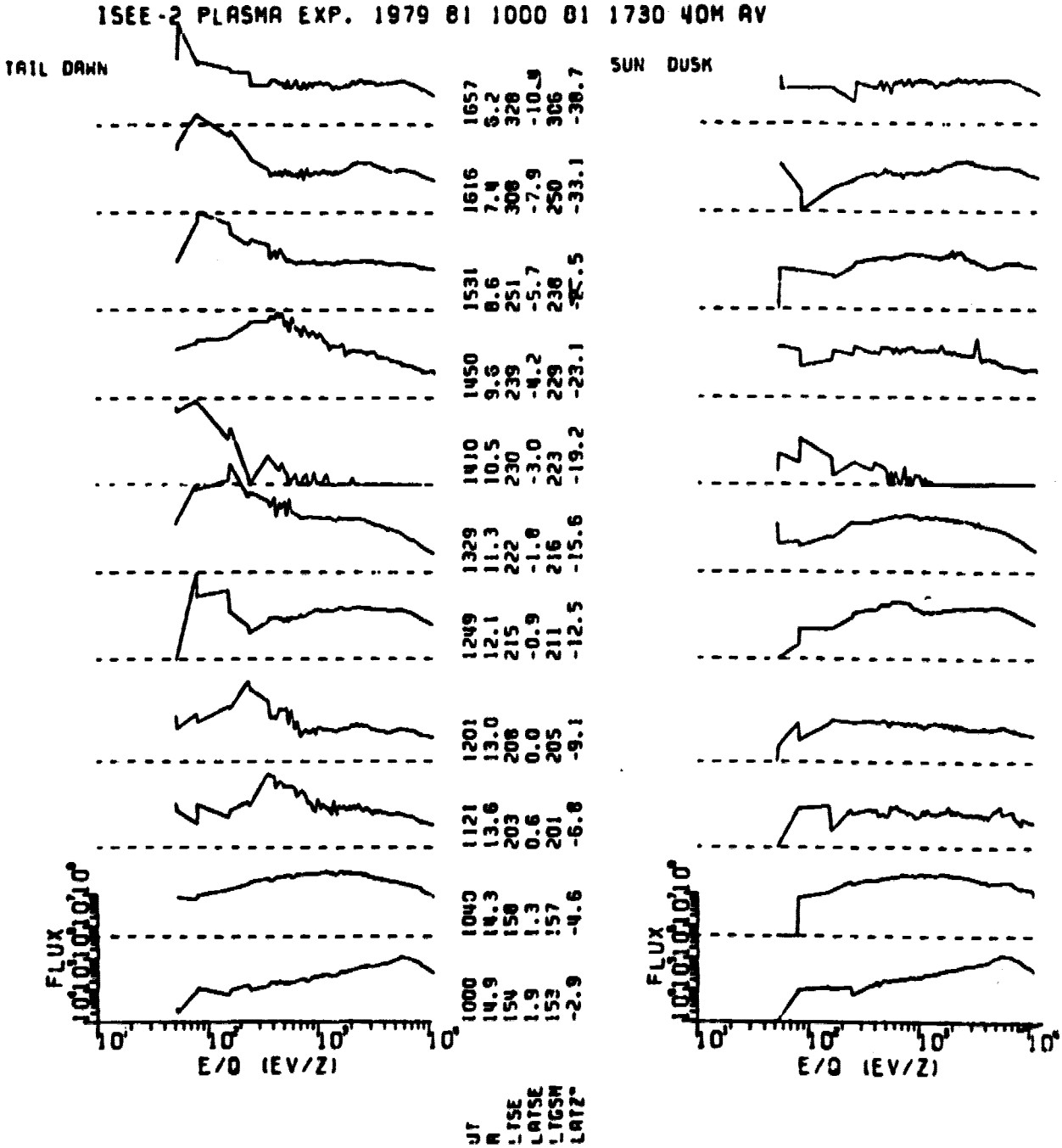
ISEE-2 PLASMA EXP. 1979 81 1000 81 1730 40M AV
TAIL DAWN
SUN DUSK
FLUX
E/Q (EV/Z)

Figure 3

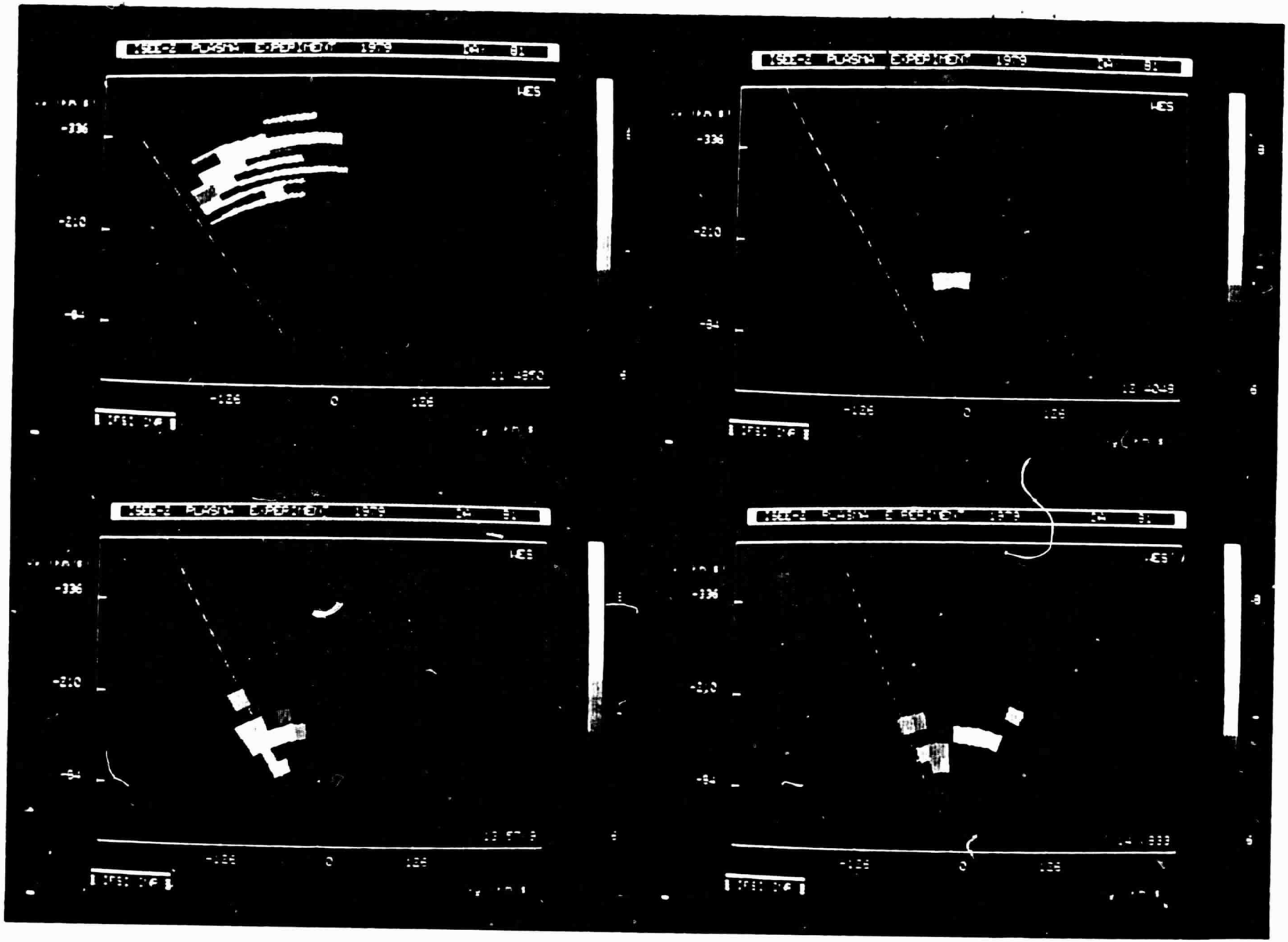

ORIGINAL PAGE IS
OF POOR QUALITY

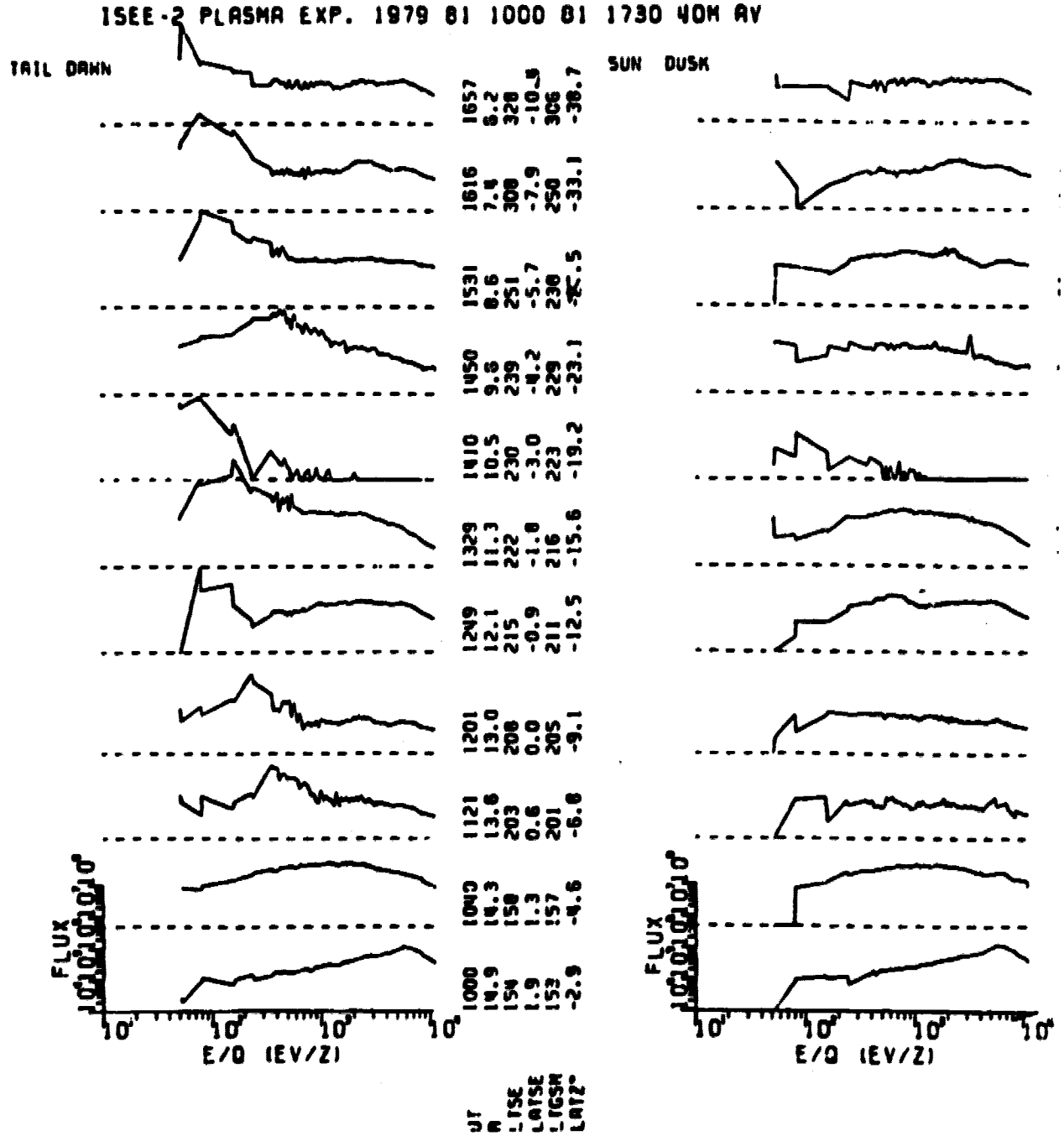

Figure 3

ISEE-2 PLASMA EXP. 1979 81 1310 81 1355 46M AV

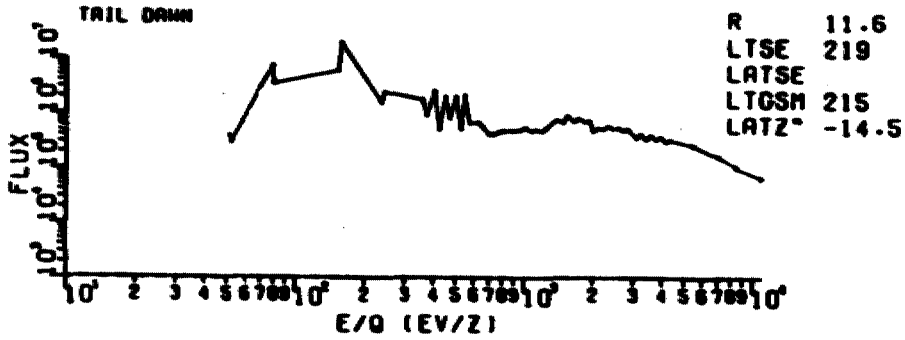

ISEE-2 PLASMA EXP. 1979 81 1610 81 1640 31M AV

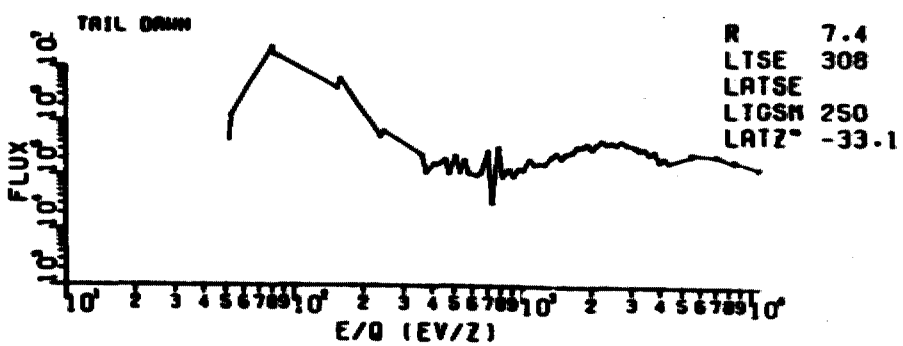

ISEE-1 ICE 1979 81 UT 1310 1354 TAIL DAWN

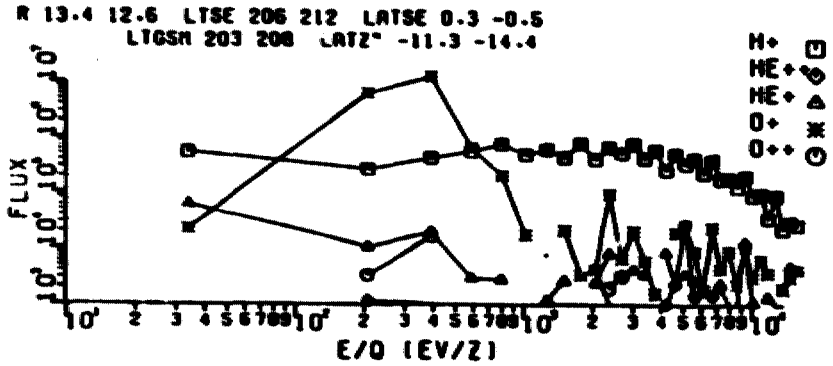

ISEE-1 ICE 1979 81 UT 1610 1640 TAIL DAWN

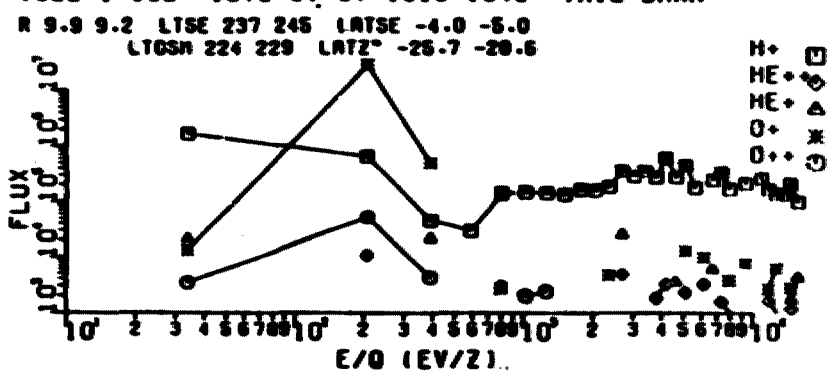

GEOS-2 / S 303 1979 81 UT 13.10 - 13.55
LT= 15.37 - 16.23

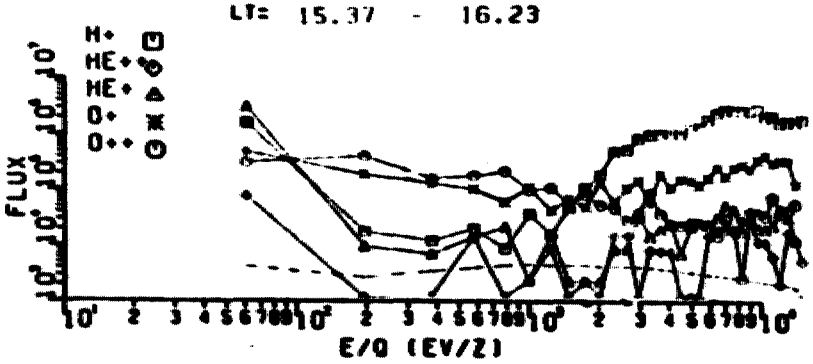

GEOS-2 / S 303 1979 81 UT 16.10 - 16.40
LT= 18.41 - 19.07

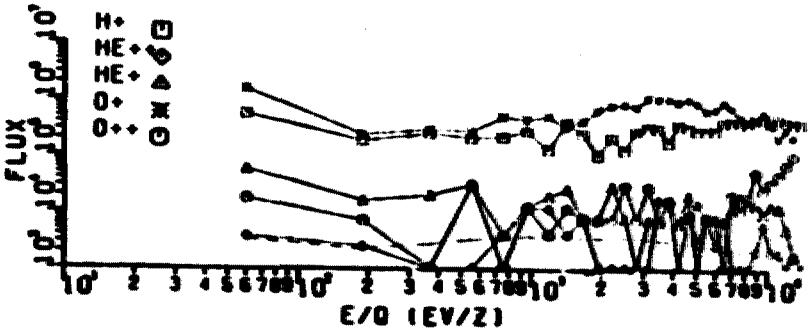

Figure 4

GEOS-2 ICE

22 MARCH 1979 ION O+

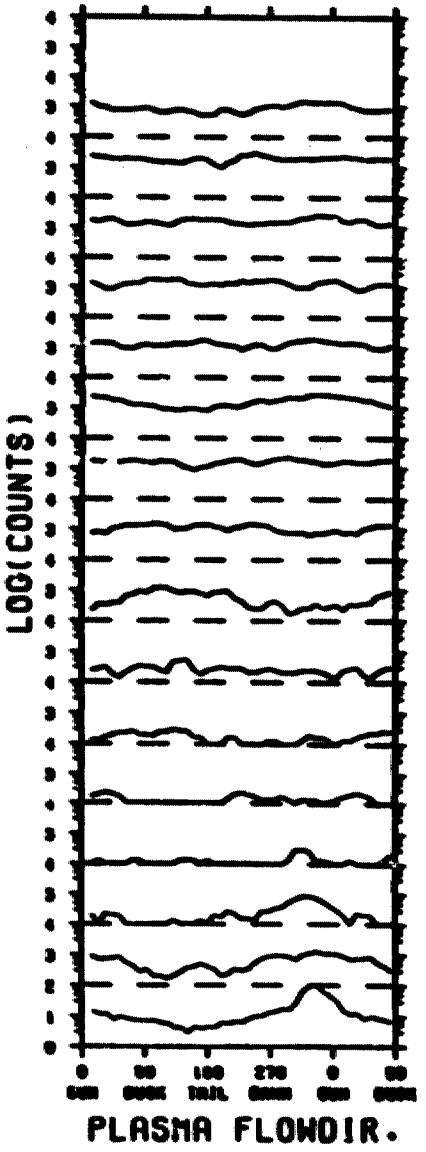

13.46 UT.
16.14 LT.
GSE:
B_X= 17.0 NT
B_Y= 31.0 NT
B_Z= 82.0 NT
GSM:
B_X= 17.0 NT
B_Y= 8.0 NT
B_Z= 88.0 NT

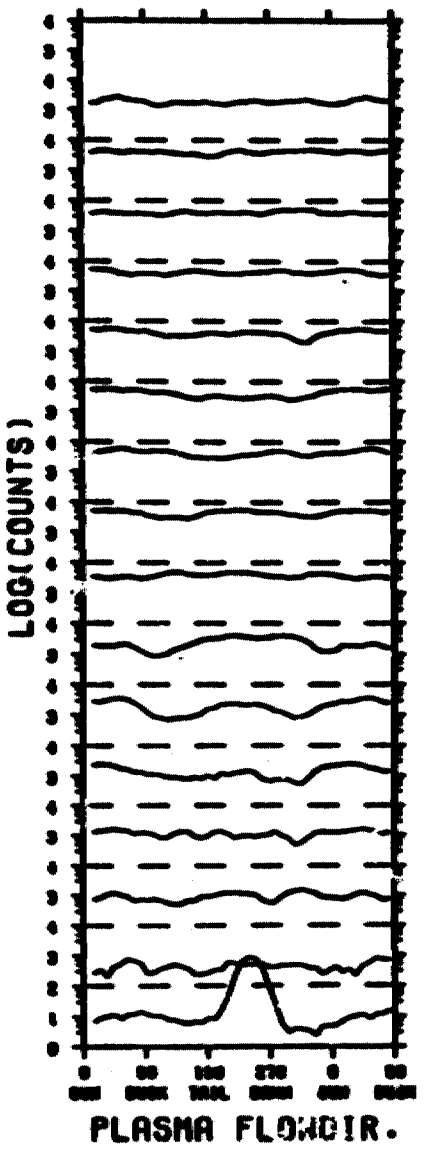

15.59 UT.
18.27 LT.
GSE:
B_X= 17.0 NT
B_Y= 45.0 NT
B_Z= 44.0 NT
GSM:
B_X= 17.0 NT
B_Y= 28.0 NT
B_Z= 58.0 NT

Figure 5

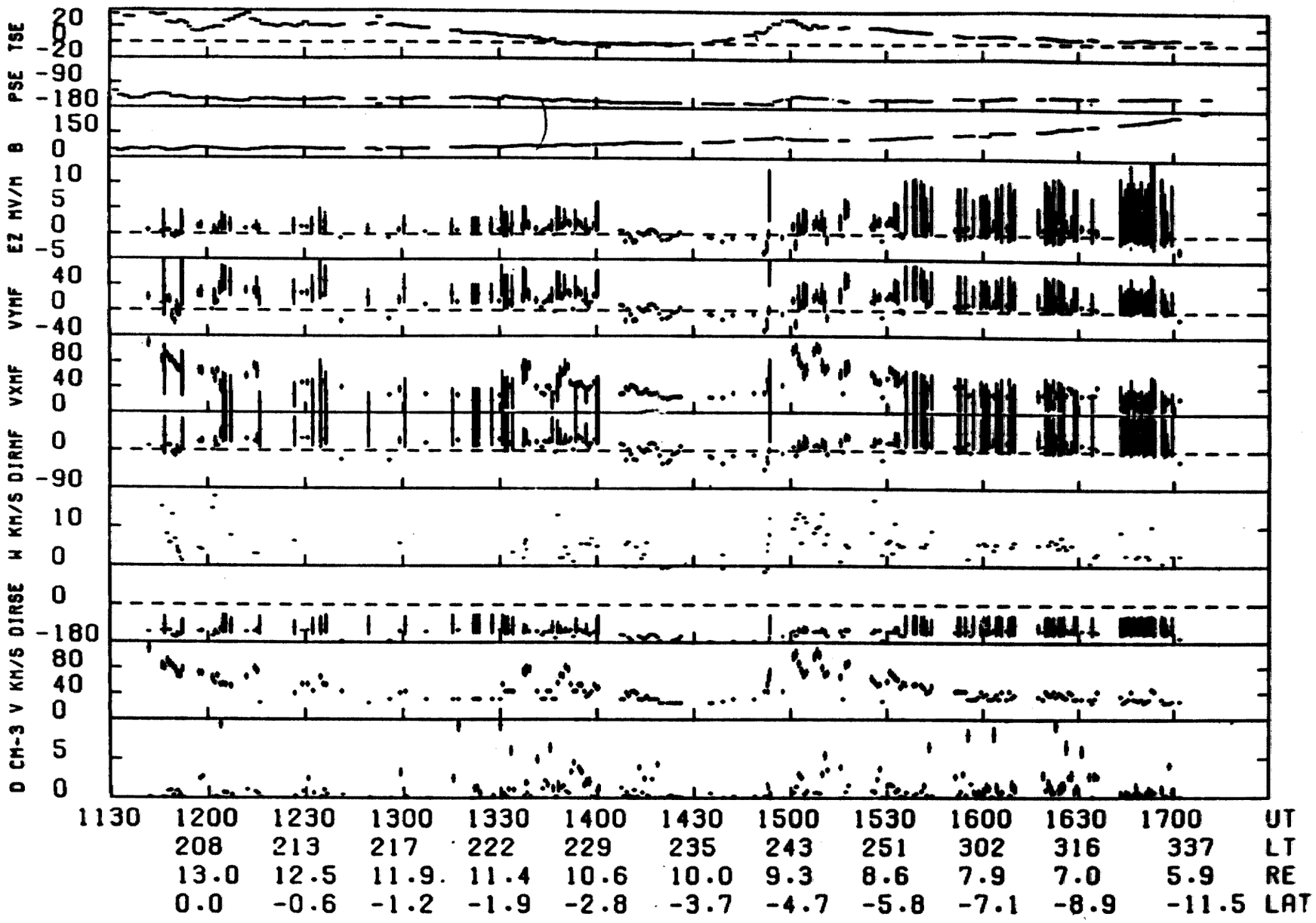
ISEE-2 PLASMA EXPERIMENT 1979 DAY 81 0+
D CM-3 V KM/S DIRSE H KM/S DIRMF VXMF VYMF EZ MV/M B PSE TSE
20
0
-20
-90
-180
150
0
10
5
0
-5
40
0
-40
80
40
0
0
-90
10
0
0
-180
80
40
0
5
0
1130 1200 1230 1300 1330 1400 1430 1500 1530 1600 1630 1700 UT
208 213 217 222 229 235 243 251 302 316 337 LT
13.0 12.5 11.9 11.4 10.6 10.0 9.3 8.6 7.9 7.0 5.9 RE
0.0 -0.6 -1.2 -1.9 -2.8 -3.7 -4.7 -5.8 -7.1 -8.9 -11.5 LAT

Figure 6

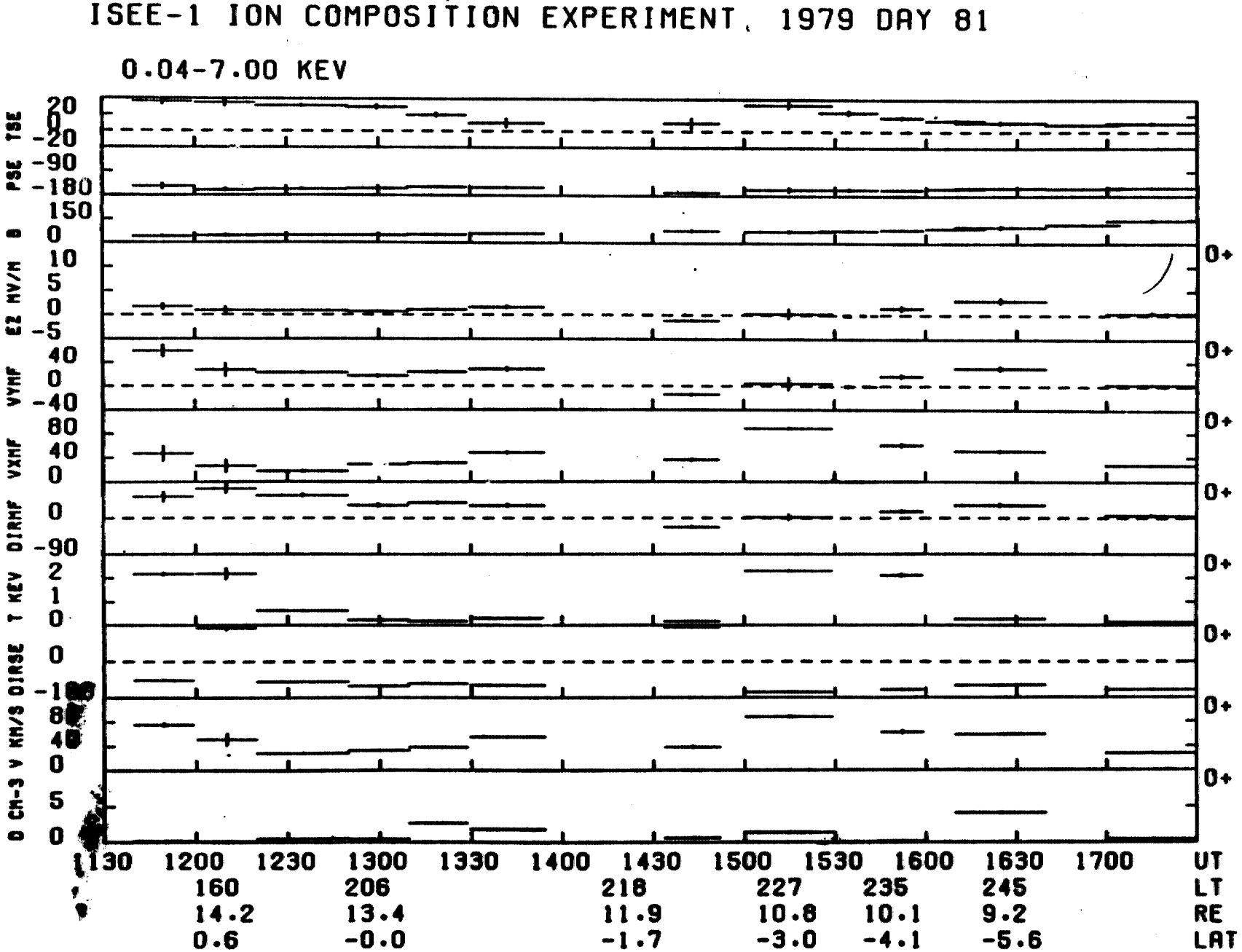
ISEE-1 ION COMPOSITION EXPERIMENT, 1979 DAY 81
0.04-7.00 KEV
PSE TSE
E2 MV/M B
VYHF
VXHF
DIRHF
T KEV
DIRSE
O CM-3 V KM/S
20
0
-20
-90
-180
150
0
10
5
0
-5
40
0
-40
80
40
0
0
-90
2
1
0
0
-1
8
4
0
0
5
0
O+
1130
1200
1230
1300
1330
1400
1430
1500
1530
1600
1630
1700
UT
160
206
218
227
235
245
LT
14.2
13.4
11.9
10.8
10.1
9.2
RE
0.6
-0.0
-1.7
-3.0
-4.1
-5.6
LAT

Figure 7

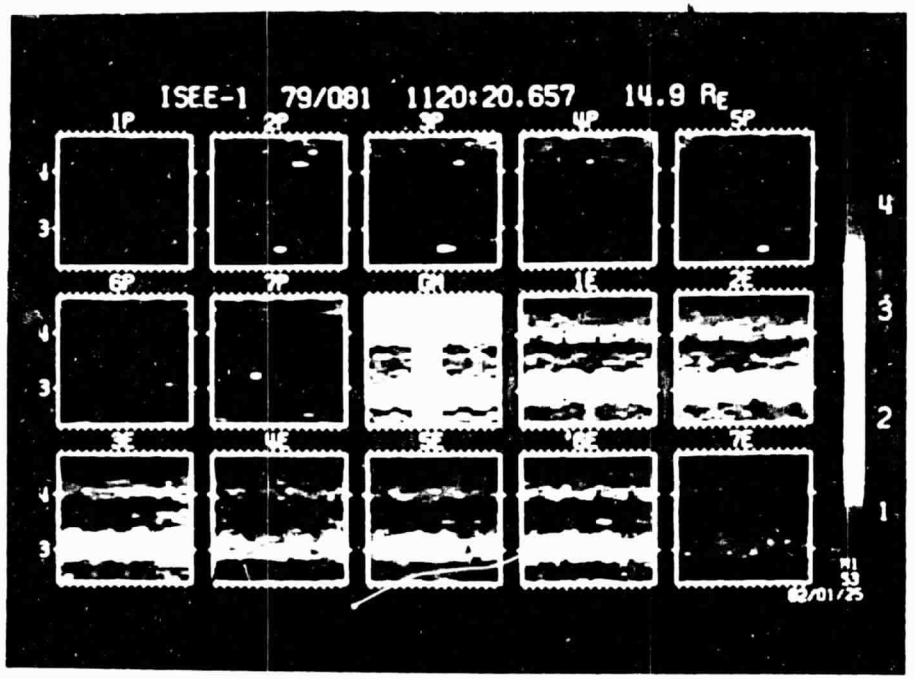
ISEE-1 79/081 1120:20.657 14.9 RE
1P
2P
3P
4P
5P
6P
7P
GM
1E
2E
3E
4E
5E
6E
7E
4
3
2
1
M1
S3
82/01/25

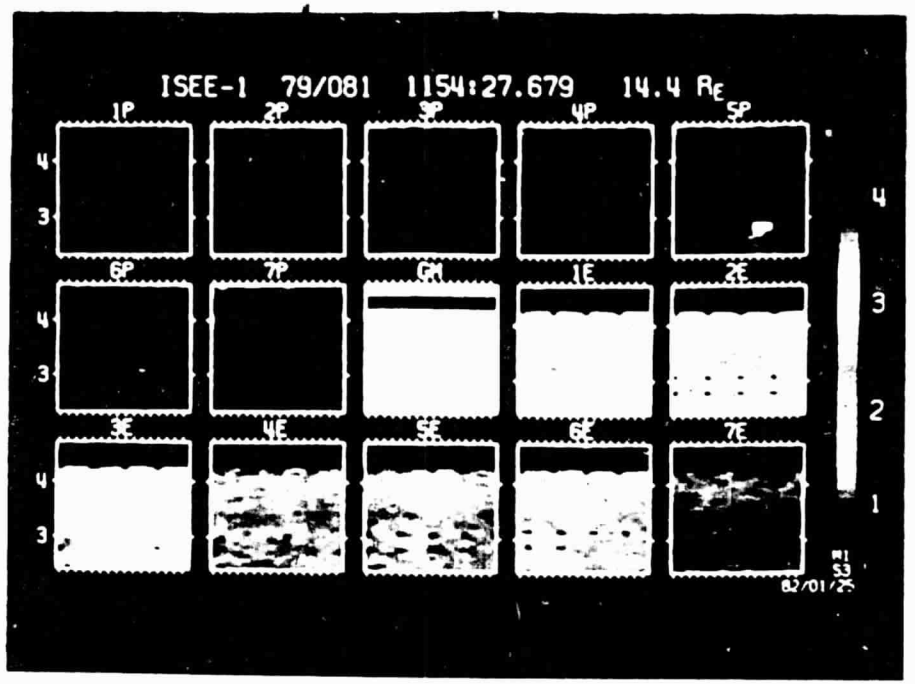
ISEE-1 79/081 1154:27.679 14.4 RE
1P
2P
3P
4P
5P
6P
7P
GM
1E
2E
3E
4E
5E
6E
7E
4
3
2
1
M1
S3
82/01/25

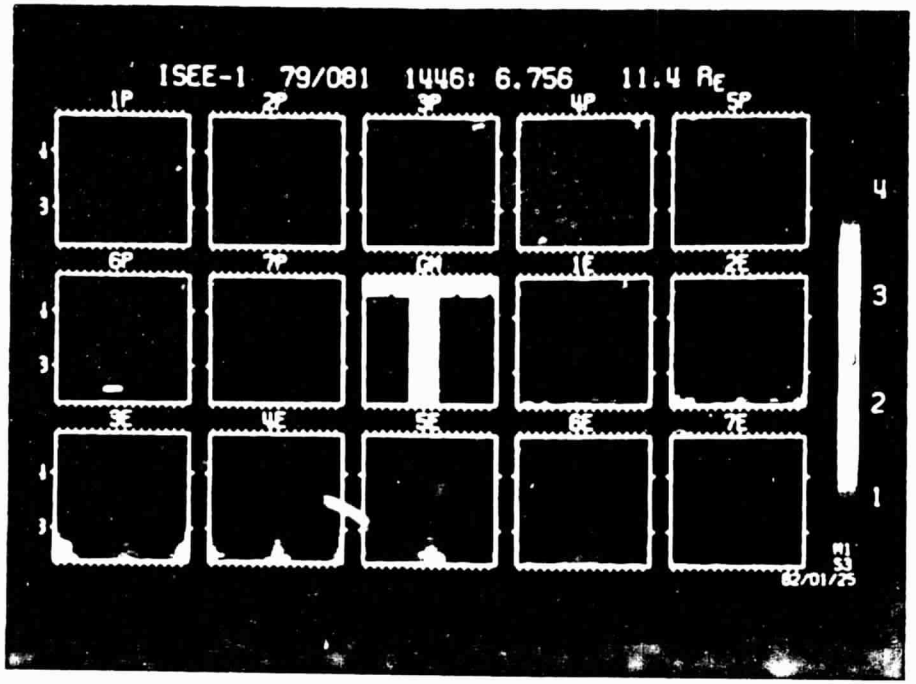
ISEE-1 79/081 1446: 6.756 11.4 RE
1P
2P
3P
4P
5P
6P
7P
GM
1E
2E
3E
4E
5E
6E
7E
4
3
2
1
M1
S3
82/01/25

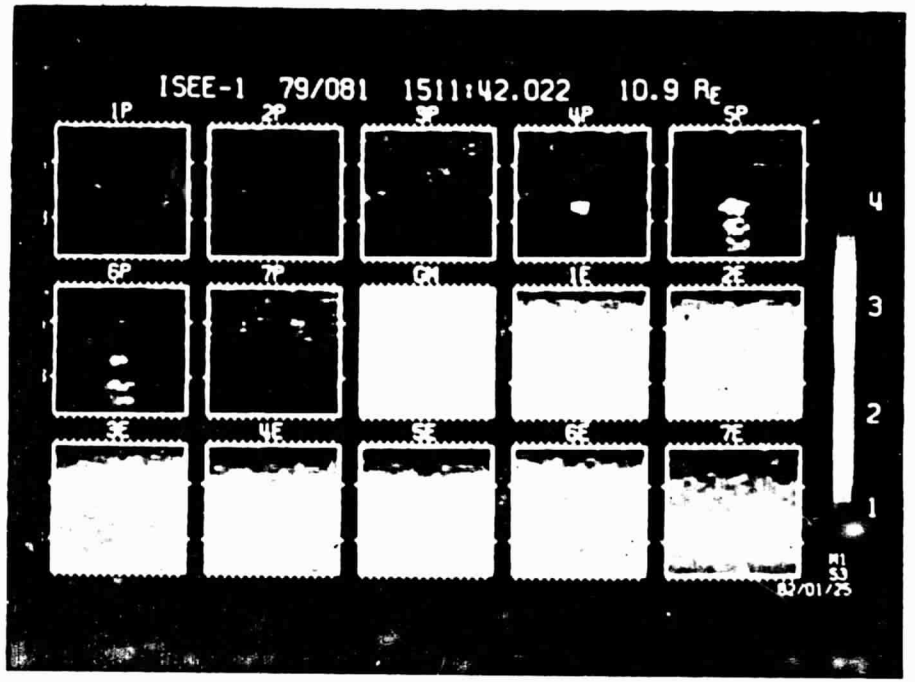
ISEE-1 79/081 1511:42.022 10.9 RE
1P
2P
3P
4P
5P
6P
7P
GM
1E
2E
3E
4E
5E
6E
7E
4
3
2
1
M1
S3
82/01/25

Figure 8

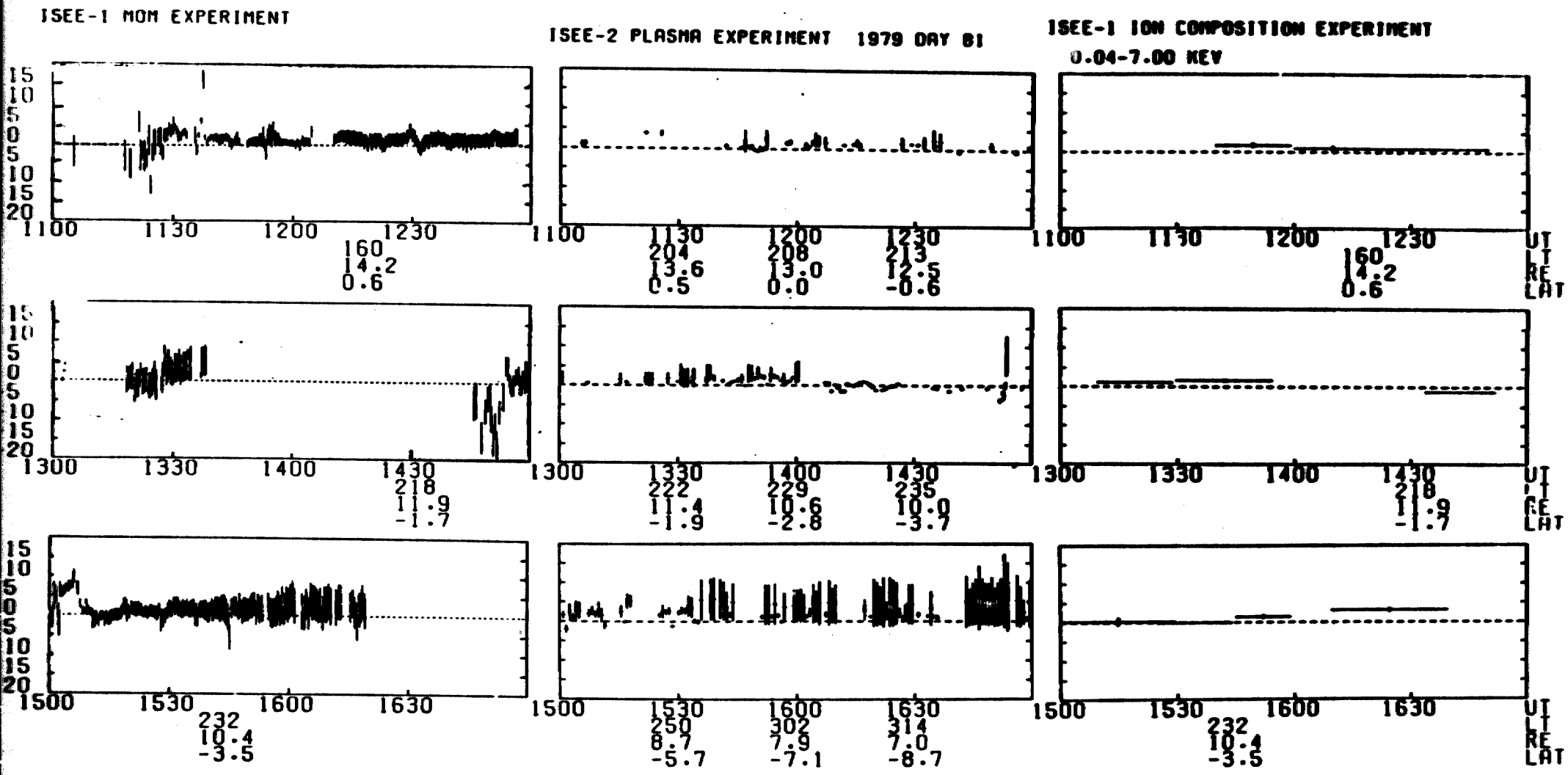
ISEE-1 MOM EXPERIMENT
ISEE-2 PLASMA EXPERIMENT 1979 DAY 81
ISEE-1 ION COMPOSITION EXPERIMENT
0.04-7.00 KEV
15
10
5
0
5
10
15
20
1100
1130
1200
1230
160
14.2
0.6
204
13.6
0.5
208
13.0
0.0
213
12.5
-0.6
UT
LT
RE
LAT
1300
1330
1400
1430
218
11.9
-1.7
222
11.4
-1.9
229
10.6
-2.8
235
10.0
-3.7
1500
1530
1600
1630
232
10.4
-3.5
250
8.7
-5.7
302
7.9
-7.1
314
7.0
-8.7

Figure 5

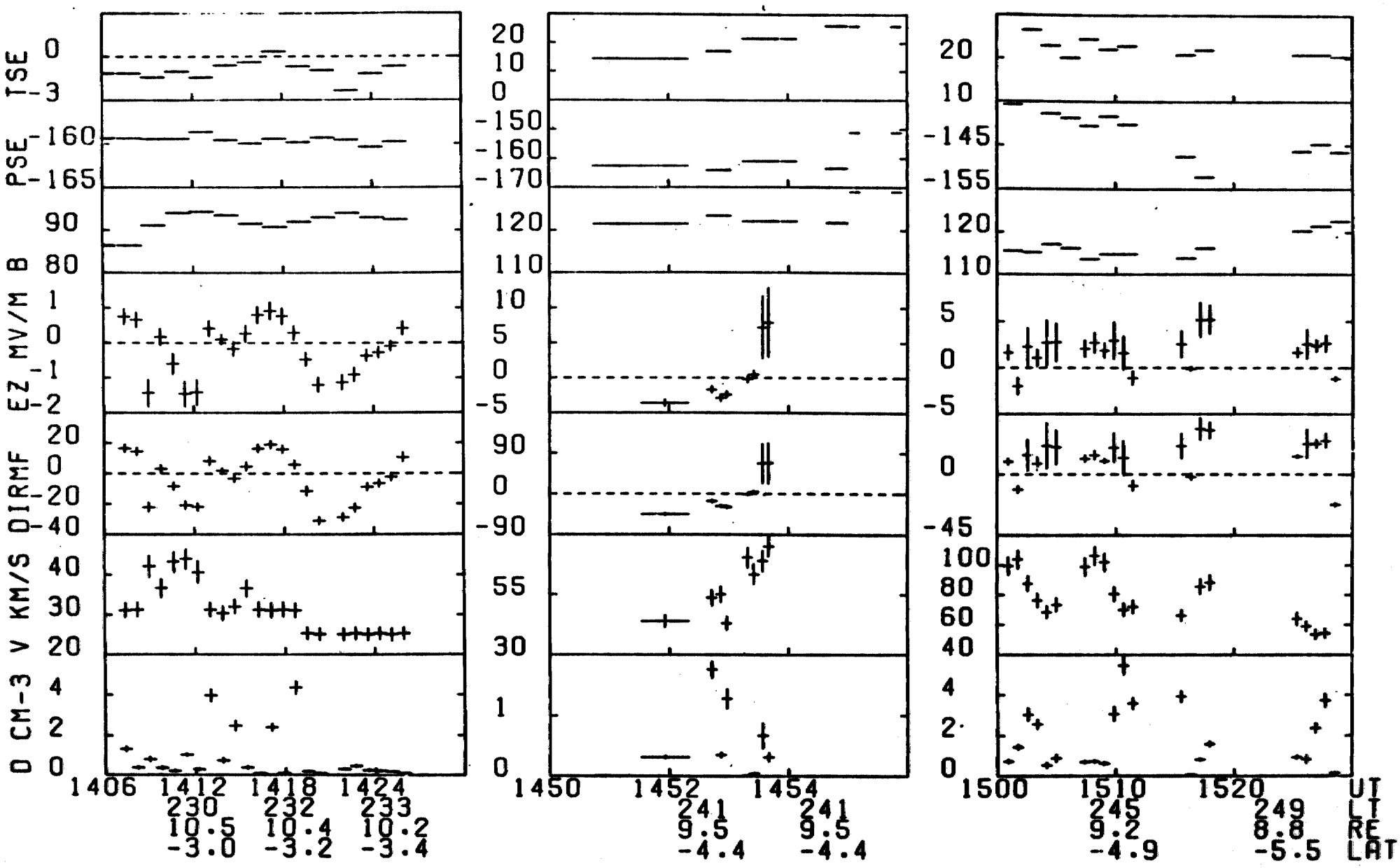
ISEE-2 PLASMA EXPERIMENT
TSE
PSE
B
EZ MV/M
DIRMF
V KM/S
D CM-3
1406 1412 1418 1424
230 232 233
10.5 10.4 10.2
-3.0 -3.2 -3.4
1450 1452 1454
241 241
9.5 9.5
-4.4 -4.4
1500 1510 1520 UT
245 249 LT
9.2 8.8 RE
-4.9 -5.5 LAT

Figure 10

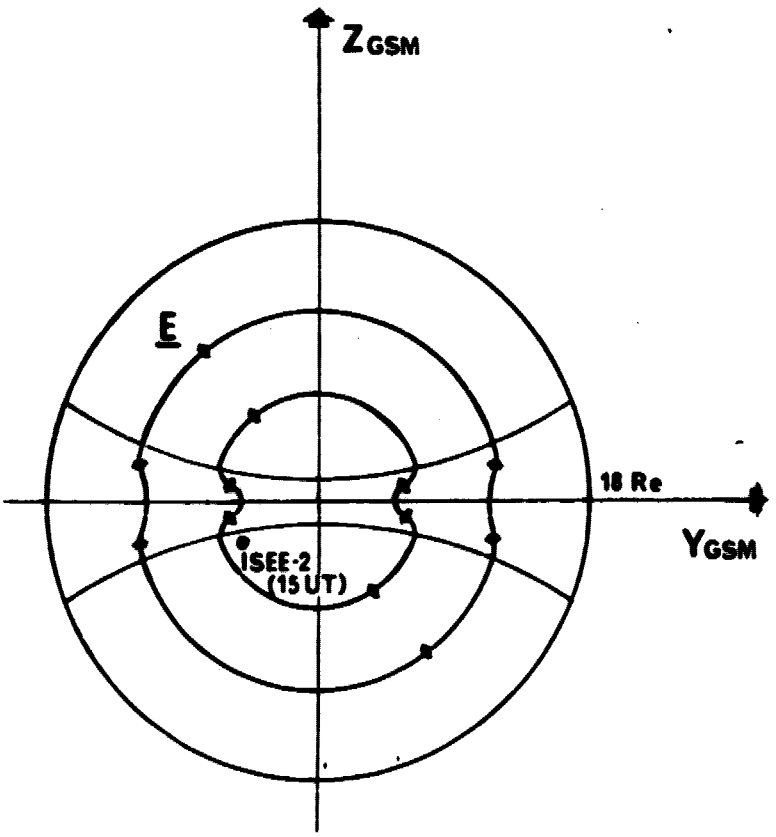

Figure 11